Proceedings of
10th European Conference on Turbomachinery Fluid dynamics & Thermodynamics
ETC10, April 15-19, 2013, Lappeenranta, Finland

LOW SPEED NUMERICAL AND EXPERIMENTAL VALIDATION OF A SOLVING METHODOLOGY FOR THE INVERSE HEAT CONDUCTION PROBLEM BY MEANS OF QUANTITATIVE INFRA-RED THERMOGRAPHY

F.Baldani [1]*, W.Bosschaerts* [1]*, S.Harmand* [2]*, T.Arts* [3]

1 Mechanics Department, Belgium Royal Military Academy, Brussels, Belgium
2 University of Lille Nord de France, UVHC, TEMPO, F-59313 Valenciennes, France
3 Turbomachinery & Propulsion Department, von Karman Institute, Rhode-saint-Genese, Belgium
Contact e-mail: francesco.baldani@rma.ac.be

ABSTRACT

The presented paper deals with the solution of the Inverse Heat Conduction Problem (IHCP) through the use of quantitative Infra Red thermography (QIRT) and proposes a solving methodology for the IHCP as a "ill-posed" problem. To solve the IHCP the surface temperature of a heat conducting body is used as boundary condition after measurement by means of an I.R. camera. The proposed methodology is first tested numerically and, subsequently, experimentally on a heated flat plate in a low subsonic speed wind tunnel. The "ill-posed" nature of the IHCP translates into a high sensibility to measurement errors, possibly leading to non-unique solutions. To reduce this sensibility a ridge regression based regularization methodology is proposed. Near-wall and free flow boundary conditions are imposed using Constant Temperature Anemometry (CTA). Results show good agreement between the proposed IHCP solution and reference cases, both for the numerical and the experimental analysis. Moreover, the proposed regularization applied for the experimental analysis is shown to enhance the accuracy of the obtained solution of the IHCP.

NOMENCLATURE

Bi:	Biot number	$\alpha_{x,y,z,t}$:	case dependent parameters $[0, 1]$
Re:	Reynolds number	$\alpha_{0,1,2}$:	Tikhonov Regularization parameters
Pr:	Prandtl number	$cond()$:	condition number
k:	thermal conductivity $[W\ m^{-1}K^{-1}]$	*Superscripts*	
C_p:	specific heat capacity $[J\ kg^{-1}K^{-1}]$	r:	iteration number
h:	heat transfer coefficient $[W\ m^{-2}K^{-1}]$	opt:	optimum
ρ:	material density $[kg\ m^{-3}]$	t:	matrix transpose
e:	electrically injected heat flux density $[W\ m^{-2}]$	p:	time step
q:	heat flux density $[W\ m^{-2}]$	*Subscripts*	
x:	coordinate in the flow direction $[m]$	meas:	measured
y:	coordinate perpendicular to the flow $[m]$	comp:	computed
ξ:	plate unheated starting length $[m]$	*Acronyms*	
th:	plate thickness $[m]$	IHCP:	Inverse Heat Conduction Problem
m,M:	discretization indices x direction	CTA:	Constant Temperature Anemometry
n,N:	discretization indices y direction	QIRT:	Quantitative Infra Red Thermography

INTRODUCTION

One of the main challenges in heat transfer study is the accurate determination of the local heat fluxes and convection coefficients, which are both often indispensable for the design of optimal and

efficient heat exchangers and not only. Examples of other applications to benefit from accurate local heat flux knowledge can be found in [13, 16, 12, 22]. The knowledge of local convection coefficients and local heat fluxes gives information on the heat transfer enhancement mechanisms. The work presented is part of a global study aiming to characterize the heat transfer from a hot surface (finned heat exchanger placed just downstream of the fan Figure 1(a), position 16), to a cold flow (main engine flow) under aircraft turbine engine conditions.

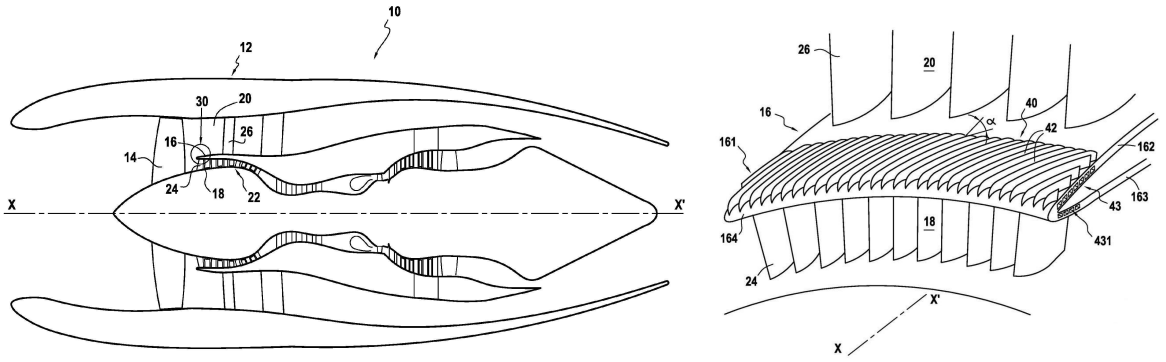

(a) Heat Exchanger Position (16)

(b) Heat Exchanger Close-up View

Figure 1: Air Cooled Oil Cooler (ACOC)
Techspace Aero Patented Design - http://www.freepatentsonline.com/EP2075194.pdf

The main difficulty encountered in the study of finned heat exchangers is the determination of the amount of heat transfer through the fin base, necessary for the calculation of fin effectiveness, without disturbing the heat flux distribution significantly. As the introduction of heat flux sensors or thermocouples between the fins and the base would introduce a thermal resistance, the heat fluxes at the fin base have to be determined indirectly by measuring the local heat fluxes through the extended surface and the primary surface [8]. Typical measurement tools are heat flux sensors, local temperature measurements or the solution of the IHCP. Since heat flux sensors introduce rather big disturbances on the heat flux distribution and are characterized by low accuracy (typically $\pm$ 10 % [23]) they are seldom used. Thermocouples are more commonly used as indirect method to determine the heat flux over a surface, and many studies use embedded thermocouples to this purpose, (for instance in [25] a technique to measure heat fluxes with two thermocouples is proposed). However, as it is applicable to one-dimensional conduction only, the method's capability is limited when measuring the heat flux distribution over a surface. Its usefulness is further limited by the number of thermocouples which can be embedded (an increased number of thermocouples interferes more and more with the heat flow, thermocouple's "fin effect" [4]). In recent years, an alternative technique has gained more popularity for identifying local heat fluxes: solve the IHCP [6]. As it already enjoys widespread use to determine heat fluxes at surfaces that are inaccessible for direct measurements [2], the solution of the IHCP was chosen as the most suitable tool for the case under analysis. Since the studied heat conducting body sits in a forced convection regime, the actual flow field is not influenced by the amount of exchanged heat injected into the flow. Therefore, as the flow field is not a priori known, it is measured using the CTA.

TRANSIENT INVERSE HEAT CONDUCTION PROBLEM

A description of the IHCP is given in [3], where it is defined as the estimation of the evolution of the surface heat flux using the measured evolution of the temperature at one or more points on a heat conducting body. Already mentioned, the main advantage of this method lies in the fact that it allows

indirect measurements where direct measurements might prove infeasible [16] or requiring expensive instruments [18]. To solve an inverse heat conduction problem, the method uses temperature measurements as input. Based on the surface temperatures of the object, the heat fluxes on the surfaces of the object can be estimated, eliminating the need for internal temperature measurements. Additionally the method allows to reconstruct the temperature distribution in the whole object, together with the coupled heat flux distribution. To minimize the disturbance of the surface temperature field and actual heat flux by the used measurement sensor, careful consideration is needed when choosing the used measurement technique. Use of embedded thermocouples will distort the temperature field of the body and may lead to a significant bias in the measurements. The errors of this distortion will propagate into the IHCP results and need to be removed through use of an appropriately detailed correction model accounting for the effect of the thermocouples [24]. However, the main disadvantage of using thermocouples is the poor spatial resolution of the temperature measurement, as only a limited number of thermocouples can be embedded. Use of Liquid Crystal Thermography (LCT) to measure the temperature can be considered [9, 15, 10], but placement of the sensors will disturb the local heat flux (possibly even the local convective boundary layer), which again will need to be compensated for [6]. For this paper, however, the setup of the experiment is prepared so that the use of QIRT was possible, eliminating any disturbance of the temperature field and at the same time allowing for a reasonably high spatial resolution. To validate the proposed method a simple geometry, a heated flat plate, is examined. The plate has length L=0.45 m, width W=0.17m and thickness th= 0.25 $\cdot 10^{-5}$ m, and is painted in matt black with a known emissivity of 0.94. The plate is heated via electric power injection and subjected to a forced convection cooling on its upper surface in a wind tunnel. As the plate is mounted in an open wind tunnel, the measured flow field over the flat plate will be used as boundary condition for the numerical simulation. Using QIRT, the measured surface temperature will be used to calculate the local convective heat transfer coefficients following the numerical IHCP solution approach ([14, 11, 7]). The general expression for the plate temperature field variation is given in eq. 1.

$$\frac{1}{th} \cdot e + k \cdot \left(\alpha_x \frac{\partial^2 T}{\partial x^2} + \alpha_y \frac{\partial^2 T}{\partial y^2} + \alpha_z \frac{\partial^2 T}{\partial z^2} \right) = \frac{1}{th} \left[q_{down} + q_{up} \right] + \alpha_t \cdot \rho \cdot C_p \cdot \frac{\partial T}{\partial t} \tag{1}$$

The plate can be considered as "thermally thin" if $Bi < 0.1$, which is the case (sketch in Figure 2), then the temperature gradient along the z direction can be neglected. The initial and boundary conditions on the plate surfaces are defined as follows:

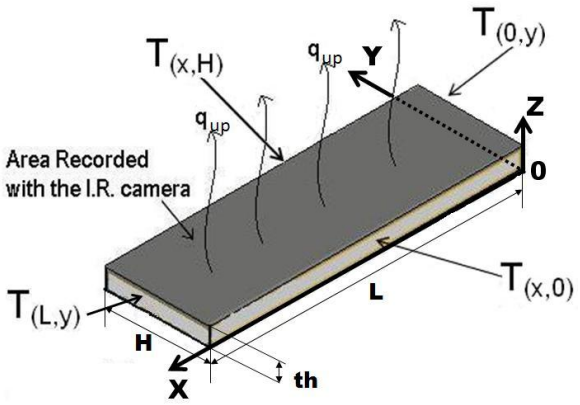

- Boundary Conditions:
  - Upper Surface: imposed $T_{surface}$
  - Lower Surface: thermally insulated ($q_{down} = 0$)
  - Side Surfaces: imposed temperatures
- Initial Condition: imposed temperature field

Figure 2: Heat Conducting Plate Sketch

In the following $q = q_{up}$. The problem reduces to the expression in eq. 2.

$$\frac{1}{th} \cdot e + k \cdot \left(\alpha_x \frac{\partial^2 T}{\partial x^2} + \alpha_y \frac{\partial^2 T}{\partial y^2} \right) = \frac{1}{th} q + \alpha_t \cdot \rho \cdot C_p \cdot \frac{\partial T}{\partial t} \tag{2}$$

Equation 2 can be used to numerically minimize equation 3.

$$F = \sum_x \sum_y \left[T_{comp}\left(x,y\right) - T_{meas}\left(x,y\right)\right]^2 \tag{3}$$

The stated problem is ill-posed and has therefore a high temperature measurement error sensitivity [3] which almost invariably leads to non-unique or erroneous results. Since the simple minimization of F has no influence on the error amplification of the input data, a regularization is proposed. Also known as ridge regression and first proposed by Tikhonov [20, 21] it can be expressed as in eq. 4.

$$S = F + \alpha_0 \cdot S_0 + \alpha_1 \cdot S_1 + \alpha_2 \cdot S_2 \tag{4}$$

Applied to the IHCP one obtains:

- F: Minimization Criterion
- S_i: Heat Flux Related Functions
  - $S_0 = \sum_x \sum_y \left[q\left(x,y\right)\right]^2$
  - $S_1 = \sum_x \sum_y \left[grad\left(q\left(x,y\right)\right)\right]^2$
  - $S_2 = \sum_x \sum_y \left[\Delta q\left(x,y\right)\right]^2$
- α_i: Regularization Parameters
  - 0^{th} Order - α_0: limits the values q_{max}
  - 1^{st} Order - α_1: limits q bigger variations
  - 2^{nd} Order - α_2: limits q quick oscillations

The main source of the measurement error in QIRT is the noise on the readout of the thermal camera, resulting in temperature readout fluctuations. As a result, only the term with order 1 will be assigned a weight as it limits these fluctuations, reducing S to eq. 5.

$$S = \sum_x \sum_y \left[T_{comp}\left(x,y\right) - T_{meas}\left(x,y\right)\right]^2 + \alpha_1 \cdot \sum_x \sum_y \left[grad\left(q\left(x,y\right)\right)\right]^2 \tag{5}$$

To find the heat flux values of next iteration step (q^{r+1}) for the minimization of S in eq. 5, the derivative of eq. 5 with respect to the fluxes of the next time step q^{p+1} needs to be zero. After rearranging the spatial discretization field into a single m by n vector, the derivative of the first part of 5 (defined as F) with respect to q^{p+1} can be expressed in matrix form as in eq. 6:

$$\frac{\partial F}{\partial q^{p+1}} = 2J.\left[T^r_{comp}(q^{p+1}) - T_{meas}\right] \tag{6}$$

where J is the temperature sensibility matrix with respect to the variation of each heat flux of the next time step p+1.

$$J = \begin{bmatrix} \frac{\partial T^r_{meas}(1)}{\partial q^{p+1}(1)} & \cdots & \frac{\partial T^r_{meas}[(M-1).(N-1)]}{\partial q^{p+1}(1)} \\ \vdots & \ddots & \vdots \\ \frac{\partial T^r_{meas}(1)}{\partial q^{p+1}[(M-1).(N-1)]} & \cdots & \frac{\partial T^r_{meas}[(M-1).(N-1)]}{\partial q^{p+1}[(M-1).(N-1)]} \end{bmatrix} \tag{7}$$

The value of $T^r_{comp}(q^{p+1})$ remains unknown but it can be calculated through a Taylor expansion of the known $T^r_{comp}(q^p)$. In matrix form it is:

$$T^r_{comp}(q^{p+1}) = T^r_{comp}(q^p) + J^t \Delta q \tag{8}$$

Combining 6 and 8 results in eq. 9:

$$\frac{\partial F}{\partial q^{p+1}} = 2J.\left[T^r_{comp}(q^p) - T_{meas}\right] + 2JJ^t\Delta q \tag{9}$$

In a similar way the derivative to q^{p+1} of the first order term S_1 in eq. 5 can be expressed in a matrix form:

$$\frac{\partial S_1}{\partial q^{p+1}} = 2X_1 q^r + 2X_1 \Delta q \tag{10}$$

where X_1 is the regularization matrix obtained deriving the discretized version of S_1 with respect to the heat flux variation. Combining eq. 10 and 9 results in 11 which is set equal to zero in order to calculate the next iteration (r+1) values for heat fluxes q^r:

$$\frac{\partial S}{\partial q} = 2J\left(T^r_{comp}(q^r) - T_{meas}\right) + 2\alpha_1 X_1 q^r + \left(2JJ^t + 2\alpha_1 X_1\right)\Delta q = 0 \tag{11}$$

Re-arranging eq. 11 to Δq^{r+1}

$$\Delta q|_{r\to r+1} = -\left(JJ^t + \alpha_1 X_1\right)^{-1}\left[J\left(T^r_{comp}(q^i) - T_{meas}\right) + \alpha_1 X_1 q^r\right] \tag{12}$$

To solve the system in eq. 12 the sensibility coefficients Q^r of matrix J need to be determined. As these coefficients represent the temperature variation caused by the flux variation for each point l they can be estimated using eq. 13

$$Q^r_l = \frac{\partial T^r_{comp}}{\partial q^{p+1}_l} = \frac{T^p_{comp}(q_l - \epsilon \cdot q_l) - T^p_{comp}(q_l)}{\epsilon \cdot q_l} \tag{13}$$

Once the matrix X_1 and the coefficients Q^r are known it is possible to determine the vector of corrections Δq which minimizes S.
The term α_1 is chosen to minimize the condition number of the solution matrix in order to minimize the sensitivity of the used system of linear equations to any errors in the data. Introducing α_1^{opt}:

$$cond\left(JJ^t + \alpha_1^{opt} X_1\right) = min\left[cond\left(JJ^t + \alpha_1 X_1\right)\right] \tag{14}$$

with $cond(\dots)$ the condition number of the solution matrix. Imposing α_1^{opt} as value for α_1 will result in the best possible conditioning of the posed mathematical problem. Returning to the inverse problem, eq. 12 is solved iteratively using α_1^{opt}. The iterative computation is stopped when the function S holds constant within an imposed tolerance interval ϵ for two consecutive iterations, and the surface heat flux q(x,y) is found. Since the surface heat flux found is the total heat flux, it can be split into its convective and radiative part:

$$q(x,y) = q_{conv.}(x,y) + q_{rad.}(x,y) = h(x,y)\left(T(x,y) - T_{ref.}\right) + \epsilon \cdot \sigma\left(T(x,y)^4 - T^4_{air}\right) \tag{15}$$

As the emissivity of the paint on the plate surface and T_{air} are both known, the convective flux at the plate surface can be determined. Using a relevant reference temperature, the local convection coefficient at each point on the surface can be computed.

IHCP SOLUTION VALIDATION

To validate the proposed IHCP methodology for calculating the local convective heat transfer coefficient, the theory will be compared to the results obtained from numerical simulations and experimental measurements.

IHCP Solution: Numerical Validation

The numerical validation is performed using commercial CFD software package ($Fluent^{©}$) and can be summarized as:

1. Compute the $h(x)$ profile via the Nusselt correlation for a heated plate with unheated starting length. Equation 16 gives the Nusselt number for a turbulent, isothermal, local flow with $Pr > 0.6$ which holds true for the imposed flow velocity (U_∞) of 9.2 m/s and bulk flow temperature (T_∞) of 18 °C.

$$Nu(x) = \frac{0.0296 \cdot Re(x)^{0.8} \cdot Pr^{1/3}}{\left[1 - \left(\frac{\xi}{x}\right)^{9/10}\right]^{1/9}} \tag{16}$$

   As some of the required fluid properties (particularly viscosity and diffusivity) have a fairly high thermal dependency, there can be some ambiguity as to which temperature should be used to compute the property values. The recommended approach is to use the film temperature, defined as the average of the wall and free-stream temperature, $T_{film} = \frac{T_{surface} + T_{air}}{2}$. After calculation of $Nu(x)$, $h(x)$ can be found directly.

2. Perform a direct simulation imposing the computed $h(x)$ in order to compute the 'hot' reference temperature field $T(x, y, t_1) = T_1$.

3. Perform a second direct simulation to compute the cooling phase and retrieve the surface 'cold' reference temperature field. $T(x, y, t_2) = T_2$.

4. Use T_1 and T_2 as IHCP boundary conditions to compute back $h(x)$

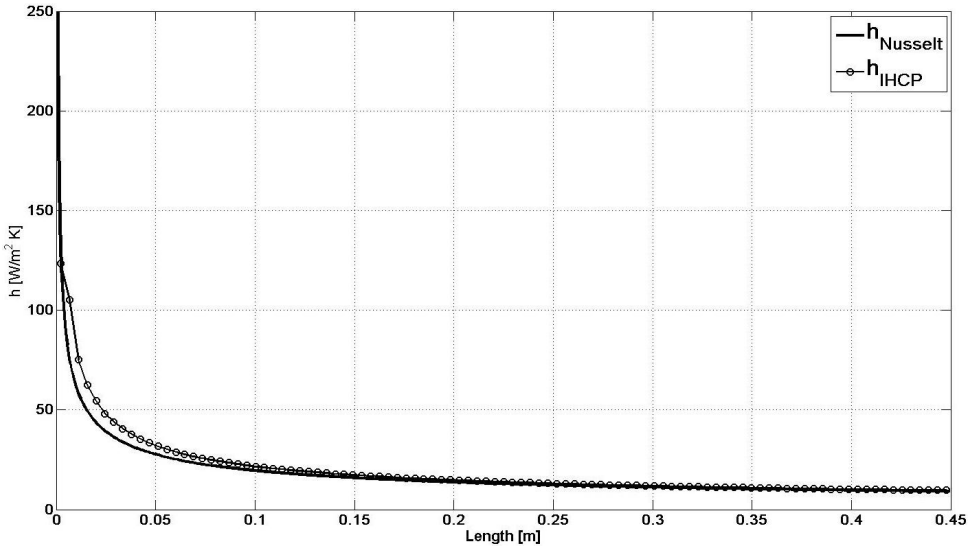

Figure 3: Theory - IHCP solution Comparison

The problem solution reported in Figure 3 shows a very good agreement with the analytical solution except at the very beginning of the plate. In this area the asymptotic nature of the Nusselt correlation used for the theory is difficult to reproduce when using discretized solutions.

IHCP Solution: Experimental Validation

The choice to exploit a heated flat plate allows an easy comparison between the experimental results and the direct numerical simulations already performed. A copper flat plate heated by an integrated electrical resistance is mounted in the test section of a low speed wind tunnel. The integrated circuit is glued on a bakelite plate placed on a polystyrene support to impose boundary conditions. Figure 4(a) and Figure 4(b) show the experimental setup and a cross section of the plate assembly. The surface temperature is measured using QIRT technique [5, 19, 17] with a *FLUKE - Ti50* I.R. camera. The camera has a 320 x 240 Focal Plane Array (FPA) and uses a vanadium oxide (VOX) uncooled microbolometer. The spectral band ranges from $8\mu m$ to $14\mu m$ with a thermal sensitivity lower than 0.070 °C at 30 °C and an accuracy of ± 2 °C or ± 2 %. It has a standard 20 mm $f/0.8$ Germanium lens with a 23°horizontal by 17°vertical field of view. The camera has a spatial resolution (IFOV) of 1.3 mrad and a minimum focus of 0.15 m. The refresh rate of the camera is 7.5 Hz. Emissivity correction is provided by user input, and ranges from 0.01 to 1 with a 0.01 step. The I.R. camera is calibrated using a black body as reference source.

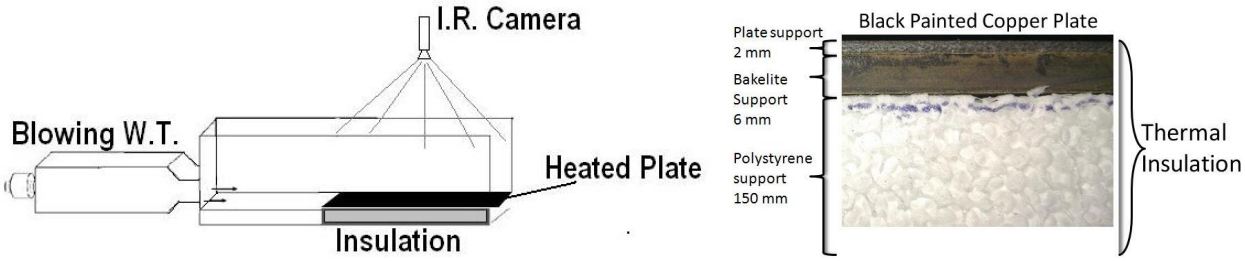

(a) Experimental Set Up Sketch

(b) Heated Plate Close Up View

Figure 4: Experimental Set Up Preparation Overview

The black body used for the camera calibration is the HGH Infrared Systems *ECN 100 blackbody*. It has a radiant surface dimension ranging from 150 mm x 150 mm to 1 m x 1 m for temperatures up to +550 °C, enabling infrared sensor calibration without collimator. The temperatures of the plate measured by the I.R. camera are benchmarked against the temperature measurement of a set of four thermocouples attached to the surface, repeated for several imposed temperatures [19]. The wind tunnel is set to have a bulk flow velocity in the test section of $9.2\ m/s$. To allow direct QIRT measurements of the flat plate, the upper part of the wind tunnel section is left open. As such, the actual flow field inside the wind tunnel has to be measured. To minimize any horizontal velocity gradients, the plate is mounted between two high vertical walls. The far field flow is measured using a *TSI* anemometer "Velocicalc Plus Air Velocity Meter". The anemometer has an uncertainty of $\pm 3\%$ of the reading or $0.015\ m/s$ with a resolution of $0.01\ m/s$ in the range from $0\ m/s$ to $40\ m/s$. The anemometer also incorporates a temperature sensor, with a resolution of 0.1 °C and uncertainty of $\pm$ 0.3 °C from -10 °C to 60 °C. To validate the turbulent boundary layer hypothesis used in eq. 16 the near wall flow is measured with a specific boundary layer hot-wire probe (Dantec 55P15 probe) connected to a Dantec Streamline 90N10 acquisition box with a 90C10 module for CTA. The boundary layer is measured in a traverse of 77 points by means of a robotized system at different heights starting from 0.025 mm. As the output of I.R. camera temperature recording is incompatible for direct input in the used IHCP solving code, the recorded images need to be adapted using a procedure given as:

1. Take any I.R. image with the color map legend present, which links the colors to the temperature levels.

2. Retrieve a vector capable to translate the R(ed)-G(reen)-B(lue) data contained in the I.R. images into a matrix containing the corresponding temperatures.

3. Translate the image into any standard $Matlab^{©}$ exploitable matrix.

4. Crop the image to the area of interest, in particular the flat plate.

Once the I.R. images are converted for the analysis, the right surface dimensions, time step and plate material characteristics should be inserted in the script. As last step to start the proposed IHCP method, the script requires the hot (T_1) and the cold (T_2) surface temperature matrices [1], which are recorded according to the the following procedure:

1. Heat the plate up to the maximum allowed temperature.

2. Start the wind tunnel and set the intended target velocity.

3. Once the velocity and the plate T_{surf} are stabilized acquire a reference surface thermograph (hot reference temperature or T_1).

4. Switch off the heating resistance.

5. After a given amount of time (Δt) record the plate T_{surf} with the I.R. camera (cold reference temperature or T_2)

RESULTS

Figure 5 shows the velocity and the turbulence intensity profiles at the heated plate leading edge, (position $x = 0\ mm$), for both the boundary layer and the free flow region. The results show that the flow field generated for the experimental campaign meets the requirements of the theoretical reference case, with Figure 5(a) showing the typical figure of a turbulent boundary layer.

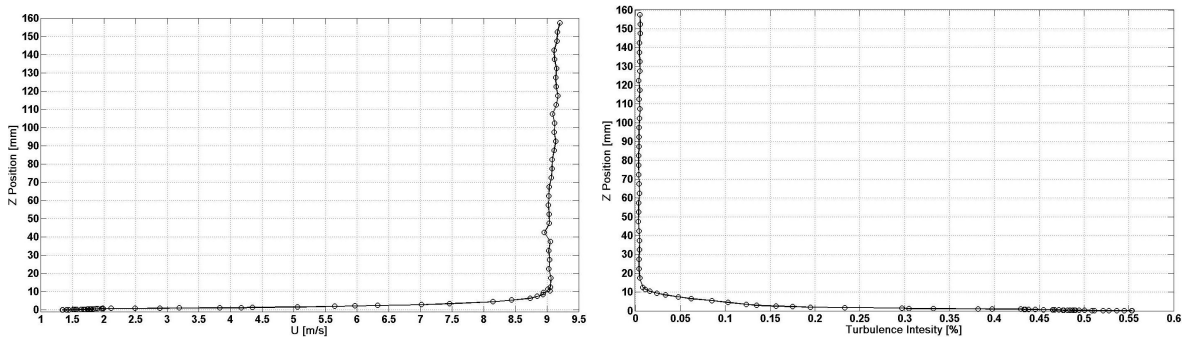

(a) Velocity Profile (b) Turbulence Intensity Profile

Figure 5: Boundary Layer Analysis

The effects of the regularization can be seen in Figure 6, where the left figure show the results of the surface temperature using the raw I.R. camera data and the contour plots on the right the resulting temperatures obtained after regularization. To illustrate the effect of the parameter α_1 on the computed surface heat flux, Figure 7 plots the computed heat transfer coefficient as a function of α_1. Additionally, the elimination of the fluctuation dampening ($\alpha_1 = 0$) shows the ill-posed character of the IHCP solution as measurements errors are amplified into large nonphysical oscillations on the calculated

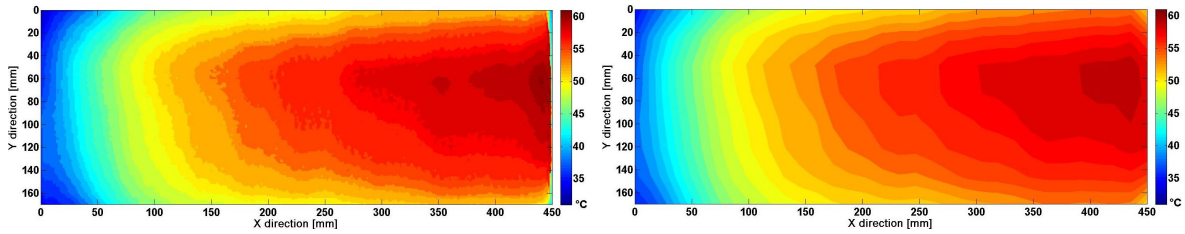

(a) T beginning - Raw data (b) T beginning - Regularization

Figure 6: Regularization Effect on the Measured Surface Temperature

heat transfer coefficient profile. Figure 7 shows that the use of α_1^{opt} gives the best estimation for the heat transfer coefficient and that higher values of α_1 will lead to the underestimation of the heat transfer coefficient. A comparison between the theory and the results of the proposed IHCP methodology is given in Figure 8. The experiment was conducted with a time step of 5.41 seconds between two I.R. images. The theory uncertainty bounds come from a 3% of relative uncertainty on U_∞, while the error for $h(x)$ mainly originates from an average 2.8% of relative uncertainty on the measured T_{surf}. The biggest discrepancy can be seen on the leading edge the plate, where the steepness of the h curve becomes problematic due to the discretization of the calculated result. Nonetheless the quality of the obtained results can be controlled by a comparison of the heat flow lost per unit distance between the theoretical and the experimental case. The lost heat flow can be computed by eq. 17 as:

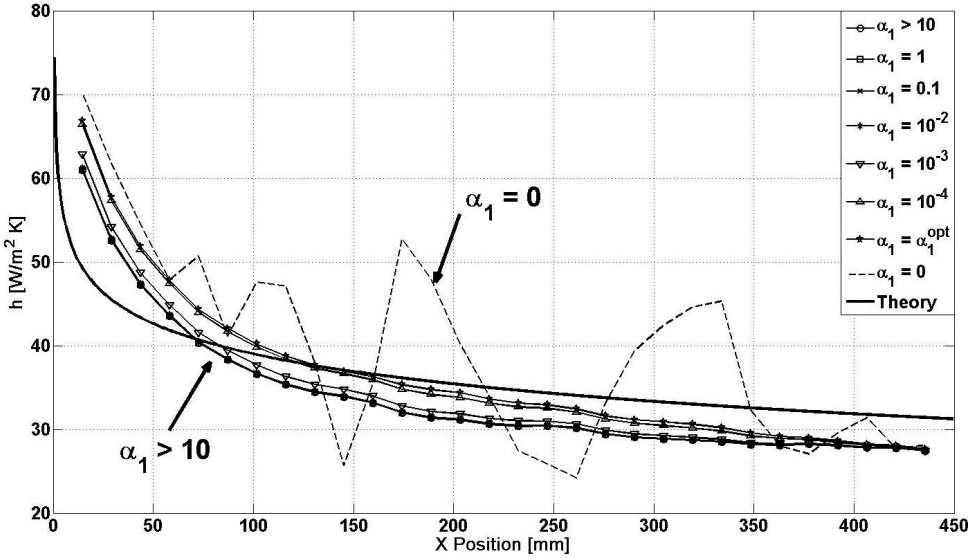

Figure 7: Regularization Effect on the IHCP Solution

$$Q = \int h \cdot \Delta T_{surf} dS \tag{17}$$

which puts the heat flow at $2.35\ W/m$ for the theory, and $2.5\ W/m$ for the experimental result.Figure 9 plots the heat transfer coefficient $h(x, y)$ for the whole plate.

CONCLUSIONS

A solving methodology for the transient inverse heat conduction problem is proposed, using infra red thermography to measure the surface temperatures. To reduce the sensibility of the IHCP solu-

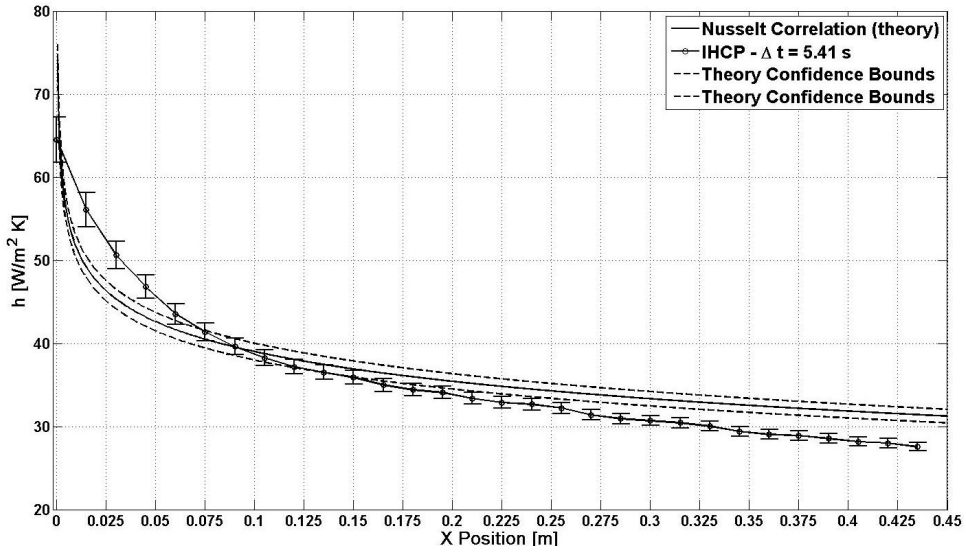

Figure 8: IHCP Solution Result - Comparison with Theory

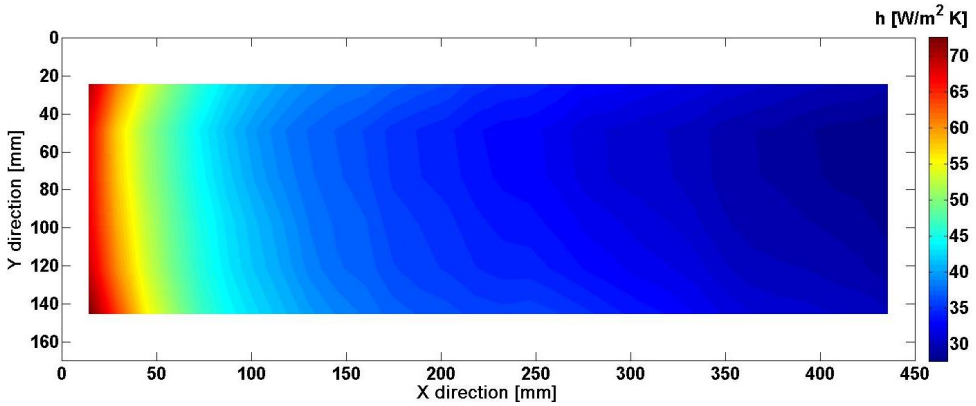

Figure 9: IHCP Solution Result - $h(x, y)$ Map

tion to the measurements noise a regularization method, based on the Tikhonov ridge regression, is applied to the specific case under analysis. The methodology is first validated numerically, using a commercial CFD code to calculate the imposed surface temperatures. A very good match between the calculated values and the theoretical Nusselt correlation results was found. An experimental validation of the proposed methodology followed. The constant temperature anemometry technique was used to characterize the flow field. The results shown a good agreement between theoretical and experimental data and proved the enhancements obtainable by applying the proposed regularization procedure, with the correct choise of parameter α_1 proven to be crucial.

FUTURE DEVELOPMENTS

A parametric study on the influence of the time interval, Δt, between the two recorded thermographs is underway. An adaptation of the proposed methodology in order to be used within a commercial CFD code is under development. This might reduce the problems encountered when discretizing part of the domain in which sudden variations of the surface heat flux might occur. Moreover the modeling of more complex geometries will be also possible. The starting approach is to propose optimization algorithms to be exploited in a CFD commercial code to subsequently implement the use of recorded surface thermographs as boundary conditions for the thermal problem.

References

[1] F. Baldani, W. Bosschaerts, and R. Wagemakers. High velocities wind tunnel flow field investigation and heat exchanger infra-red analysis. part 1: Experimental set-up, experiments and first results. *Conference Proceedings*, (ISAIF10-11), 2011.

[2] J.V. Beck, B. Blackwell, and A. Hoji-Sheikh. Comparison of some inverse heat conduction methods using experimental data. *International Journal of Heat Mass Transfer*, (Vol. 39, pp. 3649-3657), 1996.

[3] J.V. Beck, B. Blackwell, and C.R. St. Clair Jr. *INVERSE HEAT CONDUCTION - Ill-posed Problems*. International Text Books in Mechanical Engineering. Wiley Interscience Publication, first edition edition, 1985.

[4] TSZENG T. C. and SARAF V. A study of fin effects in the measurement of temperature using surface-mounted thermocouples. *Journal of heat transfer*, 125(5):926–935, 2003. eng.

[5] G. Cardone, T. Astarita, and G.M. Carlomagno. Wall heat transfer in static and rotating 180 degrees turn channels by quantitative infrared thermography. *Rev. Gén. Therm.*, (37, 644-652), 1998.

[6] P R N Childs, J R Greenwood, and C A Long. Heat flux measurement techniques. *Proceedings of The Institution of Mechanical Engineers Part C-journal of Mechanical Engineering Science*, 213:655–677, 1999.

[7] F. Coletti, A. Armellini, T. Arts, and C. Scholtes. Aero-thermal investigation of a rib-roughened trailing edge channel with crossing jets - part ii: Heat transfer analysis. *ASME paper No. GT2008 - 50695*, 2008.

[8] B. Cukurel, T. Arts, and C. Selcan. Conjugate heat transfer characterization in a ribbed cooling channel. *Conference Proceedings*, (ISAIF10 Paper nr.161), 2011.

[9] Cavallero D. and Tanda G. An experimental investigation of forced convection heat transfer in channels with rib turbulators by means of liquid crystal thermography. *Experimental Thermal and Fluid Science*, 26(2):115–121, 2002.

[10] Malay K. Das, A. Tariq, P. K. Panigrahi, and K. Muralidhar. Estimation of convective heat transfer coefficient from transient liquid crystal data using an inverse technique. *Inverse Problems in Science and Engineering*, 13(2):133–155, 2005.

[11] Pr. H Groeber and Dr. S. Erk. *Fundamentals of Heat Transfer*. McGraw-Hill Series in Mechanical Engineering. McGraw-Hill Book Company, INC., third revised edition by dr. u. grigull edition, 1962.

[12] CHEN Han-Taw, SONG Jen-Pin, and WANG Yi-Tong. Prediction of heat transfer coefficient on the fin inside one-tube plate finned-tube heat exchangers. *International journal of heat and mass transfer*, 48(13):2697–2707, 2005. eng.

[13] Cheng-Hung Huang and Hung-Chi Lo. A three-dimensional inverse problem in estimating the internal heat flux of housing for high speed motors. *Applied Thermal Engineering*, 26(14-15):1515–1529, 2006.

[14] F. Kreith. *Principles of Heat Transfer*. International Text Books in Mechanical Engineering. International Textbook Company Ltd, 158 Buckingham Palace Road London, second revised edition edition, 1965.

[15] MINGJIE LIN and TING WANG. A transient liquid crystal method using a 3-d inverse transient conduction scheme. *International journal of heat and mass transfer*, 45(17):3491–3501, 2002. eng.

[16] Alifanov O.M. and Nenarokomov A.V. Three-dimensional boundary inverse heat conduction problem for regular coordinate systems. *Inverse Problems in Engineering*, 7(4):335–362, 1999.

[17] J. Pellé and S. Harmand. Heat transfer measurement in an opened rotor stator system air gap. *Experimental Thermal and Fluid Science*, 2006.

[18] GOLBAHAR HAGHIGHI M. R., EGHTESAD M., MALEKZADEH P., and NECSULESCU D. S. Three-dimensional inverse transient heat transfer analysis of thick functionally graded plates. *Energy conversion and management*, 50(3):450–457, 2009. eng.

[19] S. Rainieri, F. Bozzoli, and G. Pagliarini. Characterization of an uncooled infrared thermographic system suitable for the solution of the 2-d inverse heat conduction problem. *Experimental Thermal and Fluid Science*, (32, pages 1492-1498), 2008.

[20] AN Tikhonov and V.Y. Arsenin. Solutions of ill-posed problems. *WH Winston, Washington, DC*, 1977.

[21] AN Tikhonov and V.Y. Arsenin. Methods for solving ill-posed problems. *Scripta Series in Mathematics (Scripta Mathematics, New York, 1977)*, 1979.

[22] CHEN Tsung-Chien, LIU Chiun-Chien, JANG Horng-Yuan, and TUAN Pan-Chio. Inverse estimation of heat flux and temperature in multi-layer gun barrel. *International journal of heat and mass transfer*, 50(11-12):2060–2068, 2007. eng.

[23] Hukseflux Website. Rc01 radiation convection heat flux sensor. `http://www.hukseflux.com/product/rc01?referrer=/product_group/heat-flux-sensors`.

[24] Jonathan W. Woolley and Keith A. Woodbury. Thermocouple data in the inverse heat conduction problem. *Heat Transfer Engineering*, 32(9):811–825, 2011.

[25] T. Wu and K. Vierow. A local heat flux measurement technique for inclined heat exchanger tubes. *Experimental Heat Transfer*, 19(1):1–14, 2006.